Effect of polarization orientation angle shift on X-band TDM SAR COSSC Product of TerraSAR-X and TanDEM-X

Asmita Gupta[a], Shashi Kumar[b], Uttara Pandey[c]
[a] School of Electronics, Devi Ahilya Vishwa Vidhyalaya , Indore
[b] Indian Institute Of Remote Sensing, Indian Space Research Organization, Dehradun
[c] IORA Ecological Solution Pvt. Ltd, Delhi

ABSTRACT

Polarization orientation angle (POA) shift in the backscattered SAR wave induced, due to irregularity of the target surface. Polarimetric signatures of the backscatter SAR wave gets affected by the POA shift, causes error in the decomposition modelling as shift in POA makes coherency matrix asymmetric. POA shift compensation is very necessary to avoid misinterpretation of decomposition modelling results. POA shift effect has been observed using coherency matrix and decomposition model results. This study is conducted over Dudhwa National Park in the state of Uttar Pradesh, using high resolution, TDM SAR COSSC Product of TerraSAR-X and TanDEM-X in Bistatic mode. Present study mainly focused on the comparative analysis of resultant scattering component of decomposition model before and after POA shift compensation. Shift in POA is investigated using circular polarization technique. Yamaguchi four component decomposition model is used to express total backscatter information in terms of volume, double bounce, surface and helix scattering. Volume scattering is overestimated however double bounce and surface scattering is under estimated in decomposition model due to POA shift present in the backscatter SAR wave. Different scattering mechanisms resulted after POA compensation were analyzed using 100 random points taken from forest structure. The results obtained by TerraSAR-X and TanDEM-X shows an overall increase in double bounce scattering and decrease in volume scattering component after POA shift compensation. It is observed that there is negligible effect of POA shift on surface scattering. POA shift compensation necessarily required to improve the accuracy of decomposition models used in the forest parameter retrieval applications.

Keywords: Polarization orientation angle (POA), synthetic aperture radar (SAR), TerraSAR-X, TanDEM-X, Yamaguchi decomposition, backscatter

1. INTRODUCTION

Synthetic aperture radar (SAR) remote sensing is an advance imaging technique used efficiently in earth monitoring applications. SAR sensor transmits microwave region of wavelengths (1mm to 1m) of electromagnetic spectrum using spaceborne or airborne platform toward earth surface. Due to microwave range of frequency SAR is more advantageous remote sensing technique over optical remote sensing as it provide day night data acquisition and dense cloud cover penetration capabilities [1]. Most used SAR wavelengths are P, L, C and X-Band. Penetration depth of SAR wave increases with the increase in wavelength. P and L-Band SAR wave penetrates deeper into the canopies as compared to C and X-Band. SAR wave coming from sensors interacts with earth surface and backscattered echoes received at sensor end. On the basis of backscattered echoes reliable information about the target surfaces is extracted. SAR data acquisition in monostatic or bistatic mode reduces the temporal decorrelation to small amount as compared to repeat pass SAR configurations[2]. In present study, dataset used is TDM SAR COSSC Product of TerraSAR-X and TanDEM-X in bistatic mode where both spacecraft fly in close orbit formation to acquire information about same footprint with different views of the target area which enables highly accurate interferograms without temporal decorrelation and atmospheric disturbances. Bistatic mode of dataset helps in obtaining the accuracy of present analysis.

SAR wave transmitted and received into four different polarization, HH, HV, VH, VV for different target structures where H is horizontally polarized wave and V is vertically polarized wave so that HV means horizontally transmitted and vertically received [3]. SAR data is discriminated into three level on the basis of polarization combination. Single polarized and dual polarized data is insufficient to provide complete backscatter information about individual scatterer present in each SAR resolution cell. Fully polarized data is able to capture all the four polarization channel HH, HV, VH and VV. Fully polarimetric data overcomes the limitation of single and dual polarized dataset with its all four polarization channel

Land Surface and Cryosphere Remote Sensing III, edited by Reza Khanbilvardi, Ashwagosh Ganju, A. S. Rajawat, Jing M. Chen, Proc. of SPIE Vol. 9877, 987726 · © 2016 SPIE
CCC code: 0277-786X/16/$18 · doi: 10.1117/12.2223704

handling capabilities. Backscatter information of fully polarimetric data is stored in the form of scattering matrix for each SAR resolution cell using all four polarization combination. Scattering matrix is a 2X2 matrix where each matrix element represents the information about individual polarization channel. Scattering matrix is proven effective for coherent targets analysis but it is insufficient for complex target structures such as vegetation. For complex target analysis, coherency or covariance matrix is to be extracted from scattering matrix. Decomposition of coherency matrix is required to classify backscattered SAR wave on the basis of distributed target structures into different scattering mechanism[4]. Scattering mechanisms are mainly volume, double bounce and surface scattering [5]. Volume scattering is mainly because of randomly oriented dipole representing canopies. Double bounce scattering is dihedral reflector representing trunk-ground interactions. Surface scattering component results from single bounce scattering i.e. wave hits the object and reflects back, it is mainly because of smooth surface or water bodies.

Decomposition models are classified into two different categories coherent and incoherent decomposition model. Several decomposition models has been developed in last few decades. Those models like freeman durdan decomposition model, proven successful to classify backscatter SAR wave into volume scattering, double bounce and surface scattering[6]. Some more scattering components are added to advance decomposition models like in four component Yamaguchi model, helical scattering component is added along with the volume, double bounce and surface scattering[7]. Backscattered wave gets affected by various geophysical properties. POA shift is zero for smooth target surfaces. For targets having some irregularities causes a shift in POA of backscattered SAR wave[8]. This shift in POA leads to misinterpretation of target structures as POA of scattering media affects the polarimetric signatures[9]. POA shift present in the backscatter data increases cross polarization intensity (HV) which make coherency matrix asymmetrical and miss evaluation of scattering component in decomposition models. POA is affected due to azimuthal and range slope as well as the radar look angle[10]. There are various techniques present for the estimation of POA, out of which Polarimetric signature and circular polarization technique are proven to be most effective [11]. POA compensation is performed by rotating the coherency matrix in order to minimize the cross polarization intensity Compensation of Shift induced in POA is very necessarily required to get accurate information about target features[12]. POA shift compensation causes variation in the resultant scattering components of Decomposition modelling mechanism. This paper is mainly focused to analyze the effect of compensating the POA shift caused due the irregular target surfaces of dense forest area in the resultant scattering mechanism of four component Yamaguchi decomposition model using high resolution X-band TDM SAR COSSC Product of TerraSAR-X and TanDEM-X in bistatic mode. Results of Four component Yamaguchi models are compared using individual scattering mechanism before and after POA shift compensation.

2. STUDY AREA AND DATA SET

2.1 Study area

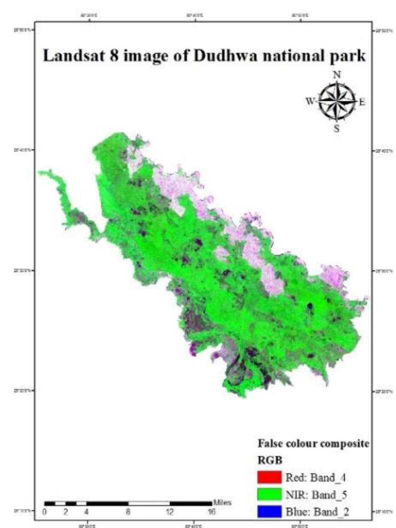

Fig. 1 FCC image of Dudhwa National park

The study area chosen for this study is Dudhwa national park located in Lakhimpur-Kheri district of Uttar Pradesh, India. Dudhwa national park, together with Kishanpur and Katerniaghat wildlife sanctuaries, represent the best natural forests and grasslands left in the Terai region of Uttar Pradesh. Dudhwa national park is a home to one of the finest Sal forests and extensive region of moist grassland. The area lies between 28° 18´N and 28° 42´N latitudes and 80° 28´E and 80° 57´E longitudes. The total area of the national park is 49029.19 ha.

Fig. 1 shows the Landsat 8 FCC imagery of the study site, where forest vegetation is well discriminated from non-forest areas. Here NIR region of EM spectrum is represented by green colour.

2.2 Data Set

Data set used are high resolution X-band, TDM SAR COSSC Product of TerraSAR-X and TanDEM-X in Bistatic mode Bistatic mode. TerraSAR-X and TanDEM-X are commercial German Synthetic Aperture Radar (SAR) Earth observation satellites, which were launched in 15 June 2007 and 21 June 2010 respectively. It has 1m resolution in spotlight mode, 2m resolution in spotlight mode, 3m resolution in stripmap mode, 18m resolution in scanSAR mode. Data acquisition was done in bistatic mode where TerraSAR-X and TanDEM-X separated by a baseline and each monostatic sensor individually recorded the information about same geometric area simultaneously in a single pass of two satellites.

Table 1. Data Specifications

Dataset	TerraSAR-X	Tandem-X
Polarization	Quad Pol	Quad Pol
Wavelength	3.108cm	3.108cm
Dimensions	7456X16030	7456X16030
Resolution	2.3334816 m	2.3340528 m
Incidence Angle	37.795 degree	37.7615 degree
Date of Acquisition	28jan2015	28jan2015
Mode of Acquisition	Strip map	Strip map

3. METHODOLOGY

Step taken in the current study described below in Fig. 2. TDM SAR COSSC Product of TerraSAR-X and TanDEM-X, are used in our study. Dataset used are in quad polarized mode. Both dataset is processed separately.

Single look complex (SLC) product data are calibrated firstly. Speckle present in the data set is reduced using improved lee sigma filter. Both dataset is having four polarization channel, HH, HV, VH and VV. Polarization channel present in the backscattered wave used to generate scattering matrix [S].

$$[S] = \begin{bmatrix} S_{HH} & S_{HV} \\ S_{VH} & S_{VV} \end{bmatrix} \tag{1}$$

Scattering matrix is a 2X2 matrix that shows the relationship between transmitted and received electromagnetic wave for a single SAR resolution cell. It is required to generate coherency matrix from the scattering matrix as it is insufficient for the analysis of complex targets such as vegetation.

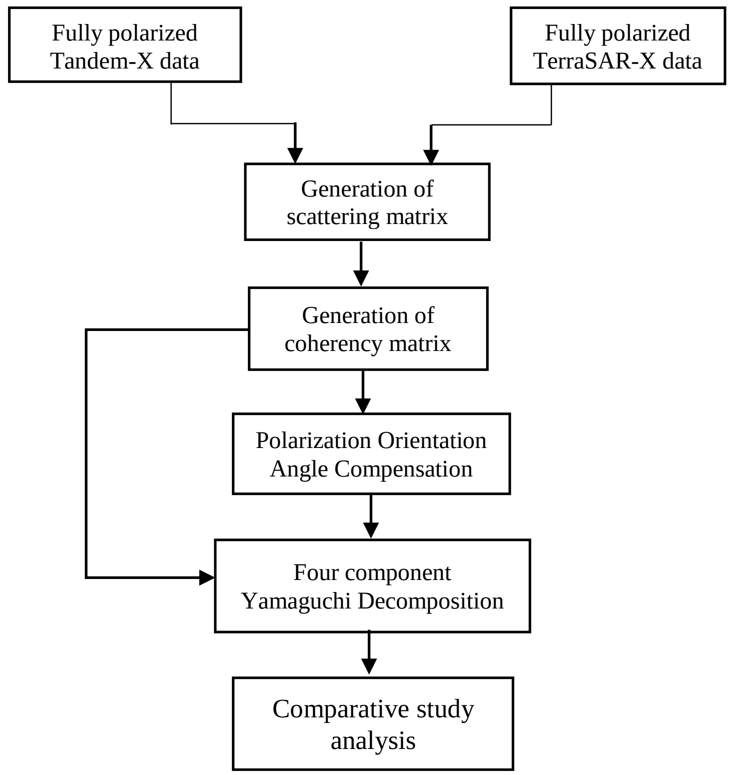

Fig. 2 Flow chart of methodology

The coherency matrix is a 3 X 3 [T] matrix that is capable to extract Polarimetric parameters of complex targets. It is generated by multiplying target vector with its complex conjugate transpose $k_p^{\dagger}$.

$$\langle[T]\rangle = \langle k_p k_p^{\dagger}\rangle \qquad \text{Where } k_p \text{ is given by} \qquad k_p = \frac{1}{\sqrt{2}}\begin{bmatrix} S_{HH+VV} \\ S_{HH-VV} \\ 2S_{HV} \end{bmatrix}^T \tag{2}$$

Coherency matrix [T] is generated as,

$$\langle[T]\rangle = \begin{bmatrix} \langle|S_{HH}+S_{VV}|^2\rangle & \langle(S_{HH}+S_{VV})(S_{HH}-S_{VV})^*\rangle & 2\langle(S_{HH}+S_{VV})S^*{}_{HV}\rangle \\ \langle(S_{HH}-S_{VV})(S_{HH}+S_{VV})^*\rangle & \langle|S_{HH}-S_{VV}|^2\rangle & 2\langle(S_{HH}-S_{VV})S^*{}_{HV}\rangle \\ 2\langle S_{HV}(S_{HH}+S_{VV})^*\rangle & 2\langle S_{HV}(S_{HH}-S_{VV})^*\rangle & 4\langle|S_{HV}|^2\rangle \end{bmatrix} \tag{3}$$

Four component Yamaguchi decomposition was performed on coherency to segregates the total power in terms of surface, double bounce, volume and helix scattering. Total power span for a single SAR pixel is equal to the sum of the individual components.

$$\langle[T]\rangle = f_s\langle[T]\rangle_{surface} + f_d\langle[T]\rangle_{double} + f_v\langle[T]\rangle_{volume} + f_c\langle[T]\rangle_{helix} \tag{4}$$

Where fs is the expansion coefficients of surface scattering, fd is for double bounce scattering, fv is for volume scattering and fc is for helical scattering. Since helix scattering is not prominent in forest areas, therefore it is not included in this study. RGB image is formed using double bounce, volume and surface scattering respectively. Decomposition results are affected by the polarization orientation angle shift as coherency matrix is de-oriented due to POA shift θ. On the basis of circular polarization technique the POA shift can be compensated by unwrapping the phase by adding π, as in

$$\eta = \frac{1}{4}\left[\tan^{-1}\left(\frac{-4\,\mathrm{Re}\,(\langle(S_{HH}-S_{VV})\rangle S_{HV}^{*}}{-\langle|S_{HH}-S_{VV}|^{2}+4\langle|S_{HV}|^{2}\rangle}\right)+\pi\right] \quad (5)$$

It is followed by

$$\theta = \begin{cases} \eta, & \text{if } \eta \le \frac{\pi}{4} \\ \eta - \frac{\pi}{2}, & \text{if } \eta > \frac{\pi}{4} \end{cases} \quad (6)$$

The coherency matrix after orientation angle rotation is obtained by

$$[\overline{T}] = [U][T][U^{T}] \quad (7)$$

Where,

$$[U] = \begin{bmatrix} 1 & 0 & 0 \\ 0 & \cos(2\theta) & \sin(2\theta) \\ 0 & -\sin(2\theta) & \cos(2\theta) \end{bmatrix} \quad (8)$$

$[\overline{T}]$ And [T] are the coherency matrices after and before rotation by POA shift θ respectively and [U] is the unitary rotation operator.

Four component Yamaguchi decomposition model is applied again on the coherency matrix after the POA shift compensation. Effect of POA shift is analysed on the basis of comparing the resultant scattering mechanism of four component yamaguchi decomposition before and after POA shift compensation.

4. RESULT

4.1 Estimated Polarization Orientation Angle (POA) shift

POA shift is calculated for TerraSAR-X and TanDEM-X dataset. Mean values and standard deviation are listed in the Table 2.

Table 2. POA shift estimated for Bistatic dataset

S. No	Data set	Mean(db)	standard deviation(db)
1	TerraSAR-X	-.0848	18.881254
2	TanDEM-X	-.6342	16.182590

It was observed that shift varies from -45° to +45° following the Gaussian distribution as shown below in the figures 3. Fig 3(A) shows POA shift in TerraSAR-X with a mean value of -.0848 db and fig 3(B) shows POA shift with a mean value of -.6342 db for TanDEM-X.

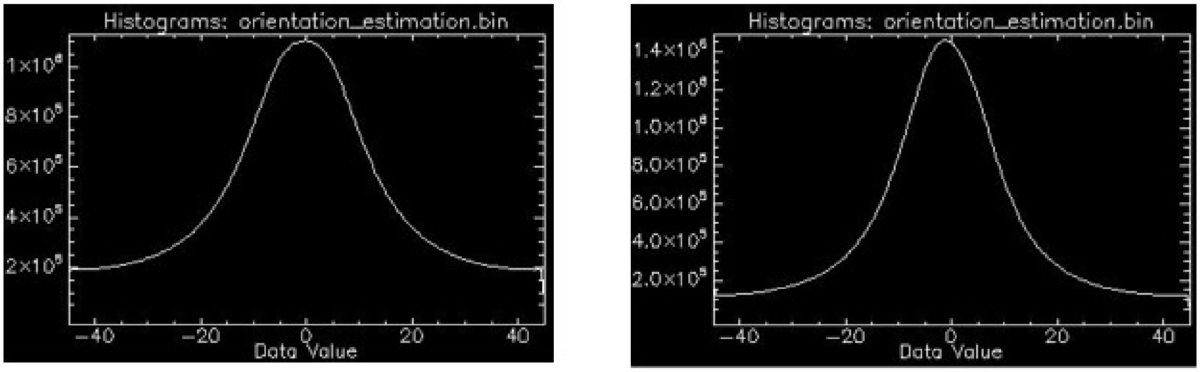

Fig. 3Histogram plots POA shift estimated using circular polarization technique
3(A). TerraSAR-X data 3(B).TanDEM-X data

4.2 Comparative analysis of before and after POA shift compensation results of Yamaguchi Decomposition

Four component Yamaguchi decomposition model results in four scattering component, volume, double bounce, surface and helix scattering. RGB image was generated by using, three scattering components of yamaguchi decomposition. Double bounce scattering corresponds to red, volume scattering corresponds to green and surface scattering is considered as blue in RGB image formation. Helical scattering is not prominent for forest area

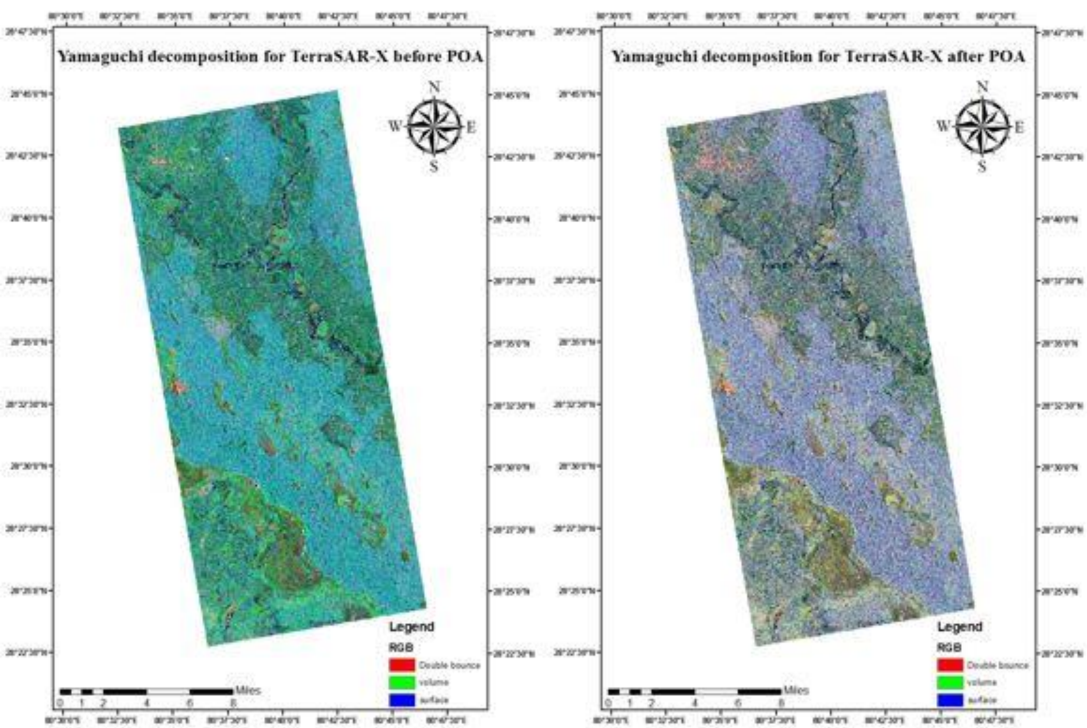

Fig 4 RGB colour coded images of Yamaguchi decomposition for TerraSAR-X (A) Before POA compensation (B) After POA compensation

Fig. 4 and Fig. 5 representing the RGB image of yamaguchi decomposition for TerraSAR-X and TanDEM-X respectively. Fig. 4(a) shows the RGB image of yamaguchi decomposition before POA shift compensation of TerraSAR-X data. Yamaguchi decomposition was performed again after compensating POA shift that can be seen in 4(b). On comparing both the images, effect of POA shift can be well noticed by observing the colour variation present in both the images. Fig 5(a) and 5(b) shows the RGB image of yamaguchi decomposition before and after POA shift compensation of TanDEM-X data respectively. POA shift was noticed on observing the colour variation present in both the images.

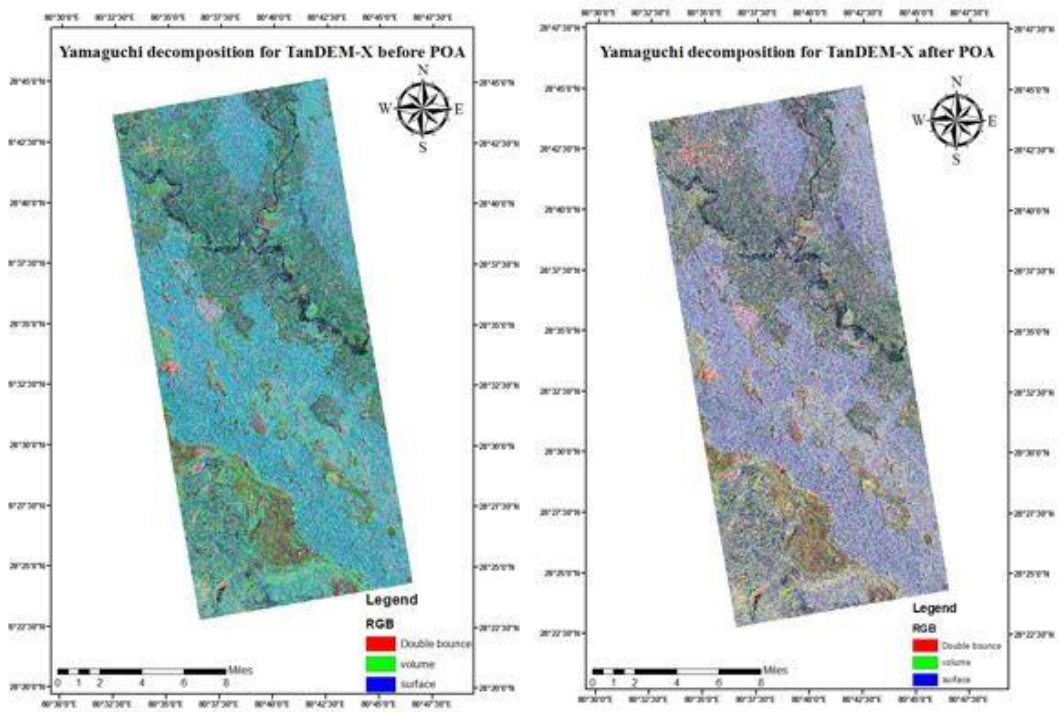

Fig 5 RGB colour coded images of Yamaguchi decomposition for TanDEM-X (A) Before POA compensation (B) After POA compensation

TerraSAR-X and TanDEM-X dataset shows difference in yamaguchi decomposition results which can be seen visually on comparing the resultant RGB images of both dataset, as shown above in fig 4 and 5.

4.3 Effect of POA shift compensation on resultant scattering component of four component Yamaguchi decomposition models

POA shift compensation produces significant impact on decomposition results. Effect of POA shift was analysed over individual scattering component derived from four component Yamaguchi decomposition for both TerraSAR-X and TanDEM-X data. In order to analyse, 100 points were randomly taken from the study area. Difference has been noticed in TerraSAR-X and TanDEM-X scattering results as shown in Table 3.

Table 3. Effect of POA shift compensation on different scattering mechanism

Data set	Double bounce scattering(dB)		Volume scattering (dB)		Surface scattering (dB)	
	Before	After	Before	After	Before	After
TanDEM-X	-15.398	-12.577	-9.257	-11.795	-7.470	-6.488
TerraSAR-X	-15.862	-12.962	-9.189	-11.967	-8.589	-7.378

It was well understood from Fig. 6 and 8, that the double bounce scattering and surface scattering, which was underestimated before was found to be increased after POA shift compensation. Double bounce scattering, increases after POA shift compensation by a mean value of -12.577dB from -15.398dB for TanDEM-X and to -12.962dB from-15.862dB for TerraSAR-X.

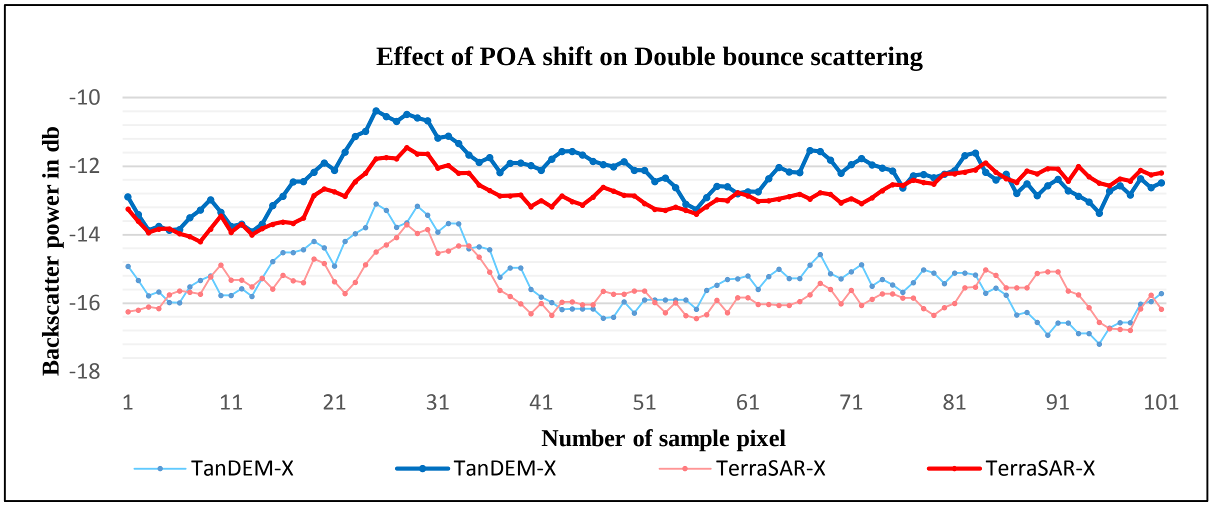

Fig. 6 Effect of POA shift compensation on Double bounce scattering component

Volume scattering component, was overestimated because of the POA shift. After compensating this shift, volume scattering component reduces to mean value of -11.795 dB from -9.257 for TanDEM-X and to -11.967dB for TerraSAR-X. Bistatic mode of TerraSAR-X and TanDEM-X shows a common behaviour of decrement in Volume scattering but with different scattering values as described in fig 7.

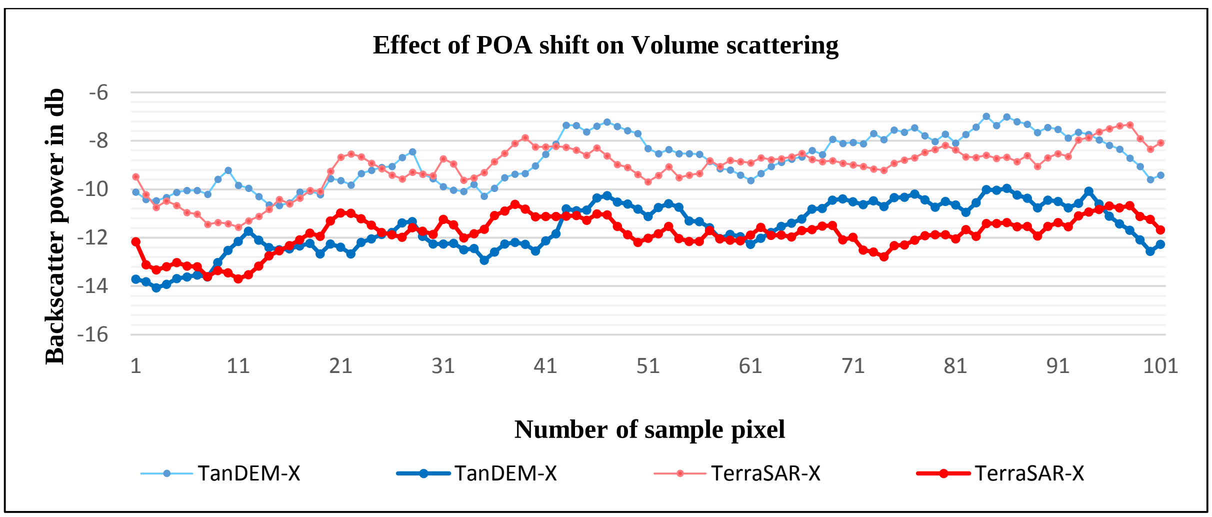

Fig. 7 Effect of POA shift compensation on volume scattering component

POA shift causes a large effect on volume and double bounce scattering component as compared to surface scattering component. Slight increase in surface scattering has been noticed in both TerraSAR-X and TanDEM-X with small difference in scattering results from both dataset as shown in fig 8. For TanDEM-X surface scattering increases to -6.488dB from -7.470 dB whereas for TerraSAR-X, it increases to -7.378dB from -8.589dB.

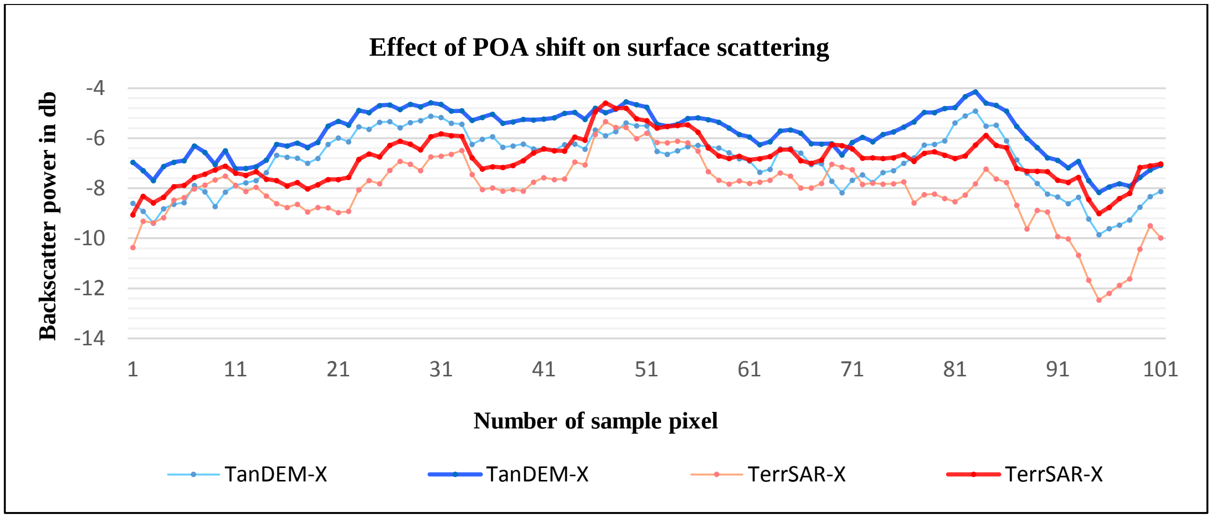

Fig. 8 Effect of POA shift compensation on surface scattering

5. DISCUSSION AND CONCLUSION

The present study mainly aims to analyze the effect of Polarization Orientation Angle (POA) shift arises in backscattered wave due to irregularity present in the target surfaces of forest structure. POA shift induced in backscattered wave affects the resultant scattering mechanisms of decomposition models. The volume scattering component get overestimated due to POA shift that will be decreased by significant amount after POA compensation. Double bounce scattering component get increased after POA shift compensation whereas a very small amount of effect was observed on surface scattering component. It is observed that accuracy of Yamaguchi four component decomposition model improves after POA shift compensation.

ACKNOWLEDGMENT

The authors are thankful to German Aerospace center (DLR) for providing TDM SAR COSSC Product of TerraSAR-X and TanDEM-X.

REFERENCES

[1] Touzi, R., Boerner, W. M., Lee, J. S.., Lueneburg, E., "A review of polarimetry in the context of synthetic aperture radar: Concepts and information extraction," Can. J. Remote Sens. **30**(3), 380–407 (2004).

[2] Nies, H., Loffeld, O., Natroshvili, K.., Kalkuhl, M., "The bistatic aspect of the TanDEM-X mission," Int. Geosci. Remote Sens. Symp., 631–634 (2007).

[3] Boerner, W.-M., Mott, H.., Luneburg, E., "Polarimetry in remote sensing: basic and applied concepts," IGARSS'97. 1997 IEEE Int. Geosci. Remote Sens. Symp. Proceedings. Remote Sens. - A Sci. Vis. Sustain. Dev. **3**, 1401–1403 (1997).

[4] Chen, S. W., Wang, X. S., Xiao, S. P.., Sato, M., "General polarimetric model-based decomposition for coherency matrix," IEEE Trans. Geosci. Remote Sens. **52**(3), 1843–1855 (2014).

[5] Han, Y.., Shao, Y., "Full polarimetric SAR classification based on Yamaguchi decomposition model and scattering parameters," Proc. 2010 IEEE Int. Conf. Prog. Informatics Comput. PIC 2010 **2**, 1104–1108 (2010).

[6] An, W., Cui, Y.., Yang, J., "Three-component model-based decomposition for polarimetric sar data," IEEE Trans. Geosci. Remote Sens. **48**(6), 2732–2739 (2010).

[7] Yamaguchi, Y., Moriyama, T., Ishido, M.., Yamada, H., "Four-component scattering model for polarimetric SAR image decomposition," IEEE Trans. Geosci. Remote Sens. **43**(8), 1699–1706 (2005).

[8] Lee, J. S.., Ainsworth, T. L., "The effect of orientation angle compensation on coherency matrix and polarimetric target decompositions," IEEE Trans. Geosci. Remote Sens. **49**(1 PART 1), 53–64 (2011).

[9] Lee, J. S., Schuler, D. L.., Ainsworth, T. L., "Polarimetric SAR data compensation for terrain azimuth slope variation," IEEE Trans. Geosci. Remote Sens. **38**(5 I), 2153–2163 (2000).
[10] Pauc, R. C., Chantrerie, L., Pottier, E., Schuler, D. L., Lee, J. S.., Ainsworth, T. L., "Estimation of the terrain surface azimuthal/range slopes using polarimetric decomposition of POLSAR data," Geosci. Remote Sens. Symp. 1999. IGARSS'99 Proceedings. IEEE 1999 Int. **4**(2), 2212–2214 (1999).
[11] Lee, J.., Schuler, D., "Polarization orientation estimation and applications: a review," Igarss, 428–430 (2003).
[12] Lee, J. Sen., Schuler, D. L., Ainsworth, T. L., Krogager, E., Kasilingam, D.., Boerner, W. M., "On the estimation of radar polarization orientation shifts induced by terrain slopes," IEEE Trans. Geosci. Remote Sens. **40**(1), 30–41 (2002).